Chiral spin liquid with spinon Fermi surfaces in the spin- $\frac{1}{2}$ triangular Heisenberg model

Shou-Shu Gong , Wayne Zheng, Mac Lee, 4 Yuan-Ming Lu, and D. N. Sheng Department of Physics, Beihang University, Beijing 100191, China Department of Physics, Ohio State University, Columbus, Ohio 43210, USA Department of Physics and Astronomy, California State University, Northridge, California 91330, USA Department of Physics, University of California, San Diego, California 92093, USA

(Received 5 June 2019; revised manuscript received 1 October 2019; published 16 December 2019)

We study the interplay of competing interactions in spin- $\frac{1}{2}$ triangular Heisenberg model through tuning the first- (J_1) , second- (J_2) , and third-neighbor (J_3) couplings. Based on a large-scale density-matrix renormalization group calculation, we identify a quantum phase diagram of the system and discover a *gapless* chiral spin-liquid (CSL) phase in the intermediate J_2 and J_3 regime. This CSL state spontaneously breaks time-reversal symmetry with finite scalar chiral order, and it has gapless excitations implied by a vanishing spin triplet gap and a finite central charge on the cylinder. Moreover, the central charge grows rapidly with the cylinder circumference, indicating emergent spinon Fermi surfaces. To understand the numerical results we propose a parton mean-field spin-liquid state, the U(1) staggered flux state, which breaks time-reversal symmetry with chiral edge modes by adding a Chern insulator mass to Dirac spinons in the U(1) Dirac spin liquid. This state also breaks lattice rotational symmetries and possesses two spinon Fermi surfaces driven by nonzero J_2 and J_3 , which naturally explains the numerical results. This realizes an example of a gapless CSL state with coexisting spinon Fermi surfaces and chiral edge states, demonstrating the rich family of interesting quantum phases emergent from competing interactions in triangular-lattice magnets.

DOI: 10.1103/PhysRevB.100.241111

Introduction. Quantum spin liquids (QSLs) are novel quantum phases of matter, which do not exhibit any symmetrybreaking orders even at zero temperature [1-3] but feature long-range entanglement and fractionalized excitations [4–7]. OSLs have been studied extensively in the past few decades, due to their important role in understanding strongly correlated materials and potential application in topological quantum computation [8–12]. While gapped QSLs have been classified and characterized systematically, there is much less understanding on gapless QSLs and how they could be realized in materials. Although a gapless QSL with Dirac cones of spinons has been shown to exist in the exactly soluble Kitaev model [12], so far there is no definitive evidence that a Dirac spin liquid has been realized in any magnetic materials [2,13]. A more exotic state is the gapless QSL with spinon Fermi surfaces (SFSs) [14–16]. Such a QSL has an extensive number of low-energy excitations, and was shown to be stabilized by four-spin ring-exchange couplings that can arise from strong charge fluctuations in weak Mott insulators [17–21].

Experimentally, many QSL candidate materials fall into the family of layered spin- $\frac{1}{2}$ magnets on the triangular lattice, such as the organic salts [22–26] and the transition-metal dichalcogenides [27–30]. Specific heat and thermal transport measurements point towards the presence of extensive mobile gapless spin excitations, which appear to be consistent with a gapless QSL with SFSs [24,26,28]. These materials are considered to be weak Mott insulators with strong charge fluctuations, which may induce such gapless QSL behaviors [17–21]. However, a direct study on the triangular Hubbard model suggests a possible gapped chiral spin-liquid (CSL)

phase in the intermediate U region [31]. Therefore, a clear theoretical understanding of the mechanism to realize gapless QSLs in these layered quasi-two-dimensional magnets is still lacking.

Another route to QSL is through competing interactions between different neighboring sites, such as the kagome compound kapellasite [32] and J_1 - J_2 - J_3 kagome model [33,34]. Recently, competing interactions have also been found essential to understand possible QSLs in the triangular-lattice rare-earth compounds [35–39] and delafossite oxides [40–43]. Indeed, a QSL phase has been found in the spin- $\frac{1}{2}$ J_1 - J_2 triangular Heisenberg model (THM) although its nature has not been established [44–51]. Therefore, understanding how QSL phases emerge from competing interactions is an important issue in order to discover new QSL materials [52–54].

In this Rapid Communication, we systematically study the spin- $\frac{1}{2}$ J_1 - J_2 - J_3 THM using the density-matrix renormalization group (DMRG) method and the parton construction. The model Hamiltonian is given as

$$H = J_1 \sum_{\langle i,j \rangle} \mathbf{S}_i \cdot \mathbf{S}_j + J_2 \sum_{\langle \langle i,j \rangle \rangle} \mathbf{S}_i \cdot \mathbf{S}_j + J_3 \sum_{\langle \langle \langle i,j \rangle \rangle \rangle} \mathbf{S}_i \cdot \mathbf{S}_j, \quad (1)$$

where J_1, J_2, J_3 are the first-, second-, and third nearest-neighbor (NN) interactions as shown in the inset of Fig. 1(a). We choose $J_1 = 1.0$ as the energy scale. In the coupling range $0 \le J_2/J_1 \le 0.7$, $0 \le J_3/J_1 \le 0.4$, besides the previously found J_1-J_2 spin liquid and different magnetic orders, we identify another gapless CSL phase as shown in Fig. 1(a). This CSL state spontaneously breaks time-reversal symmetry

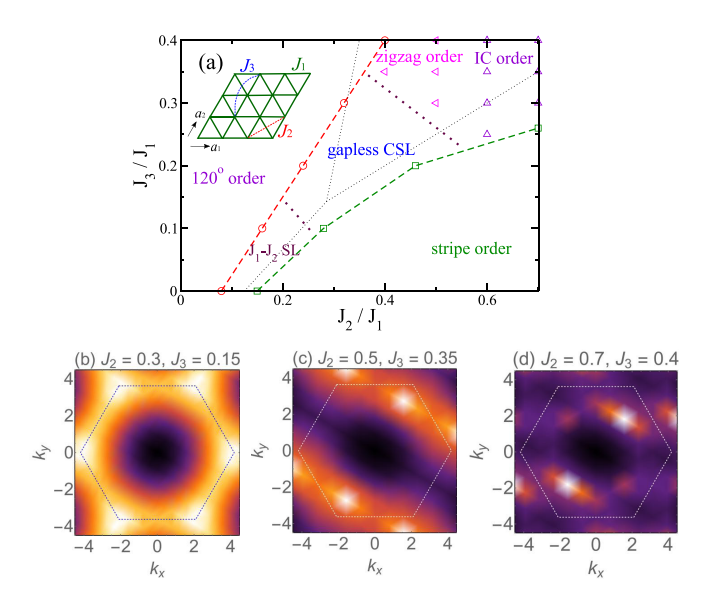


FIG. 1. Quantum phase diagram of spin- $\frac{1}{2}$ J_1 - J_2 - J_3 THM. The inset shows the model on the YC geometry. We find a 120° order, a stripe order, a zigzag order, an incommensurate (IC) order, and a gapless chiral spin-liquid (CSL) phase in the neighbor of the previously found J_1 - J_2 spin-liquid (SL) phase. The colored dotted lines are schematic phase boundaries, and the black dotted lines are the classical phase boundaries of the 120°, stripe, and zigzag orders. Static spin structure factors of the gapless CSL (b), the zigzag state (c), and the incommensurate state (d) on the YC8 cylinder.

(TRS) with a finite scalar chiral order. We also observe spin pumping upon flux insertion, similar to the charge pumping in Laughlin-type fractional quantum Hall states, indicative of a chiral edge mode, which is further confirmed by the entanglement spectrum. Finite-size scaling of the spin triplet gap on the squarelike clusters shows a vanished spin gap. The gapless nature is further supported by the bipartite entanglement entropy, which exhibits a logarithmic correction of the area law versus subsystem length, leading to a finite central charge. The central charge grows with the cylinder circumference consistent with a QSL with emergent SFSs. We propose a staggered flux state in the Abrikosov-fermion representation of spin- $\frac{1}{2}$ operators, which explains the coexistence of the chiral edge mode and SFSs observed in this gapless CSL.

We study the system by using DMRG with SU(2) symmetry [55,56]. We use cylinder geometry with periodic boundary conditions along the circumference direction and open boundary conditions along the extended direction. The lattice vectors are defined as $\mathbf{a}_1 = (1,0)$ and $\mathbf{a}_2 = (\frac{1}{2},\frac{\sqrt{3}}{2})$. Two geometries named YC and XC cylinders are studied, both having extended directions along \mathbf{a}_1 . For the YC and XC cylinders, the circumference direction is along \mathbf{a}_2 and perpendicular to \mathbf{a}_1 , respectively. The cylinders are denoted as YCL_y-L_x and XCL_y-L_x with L_y and L_x being the numbers of sites along the circumference and extended directions. We study the systems with $L_y = 5$ –12 by keeping up to 8000 SU(2) states [equivalent to about 24000 U(1) states] to obtain accurate results with truncation error less than 10^{-5} in most calculations.

Quantum phase diagram. We demonstrate the quantum phase diagram in Fig. 1(a). With growing J_2 and J_3 , we find

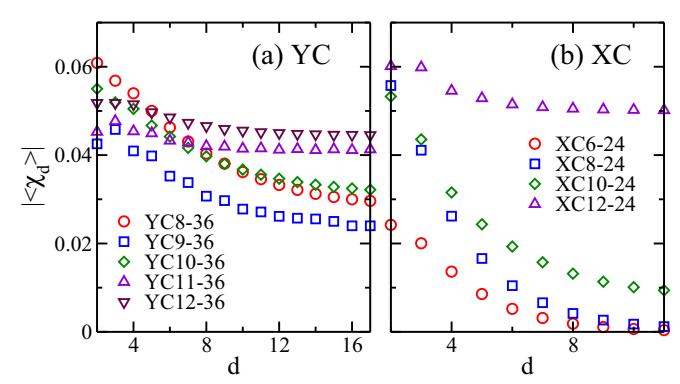


FIG. 2. Finite scalar chiral order of the CSL state at $J_2 = 0.3$, $J_3 = 0.15$. (a) and (b) are the scalar chiral orders measured from the boundary to the bulk on the YC and XC cylinders. The scalar chiral order $\langle \chi \rangle = \langle \mathbf{S}_1 \cdot (\mathbf{S}_2 \times \mathbf{S}_3) \rangle$ is defined for the three spins \mathbf{S}_i (i = 1, 2, 3) for each triangle, and d is the distance of the triangle from the edge. The chiral orders of all the triangles have the same chiral direction.

different magnetically ordered phases and QSL phases. In Fig. 1(a), the black dotted lines denote the classical phase boundaries of the 120° , stripe, and zigzag orders. We also find an incommensurate (IC) magnetic order in the neighbor of the zigzag order, consistent with previous spin-wave calculations [52]. The incommensurate order might be considered as the zigzag order with an incommensurate modulation (see Supplemental Material [57]). In the presence of quantum fluctuations, we find another gapless CSL phase near the triple point of the classical orders, which sits at the neighbor of the J_1 - J_2 SL. By computing spin and dimer correlation functions, we find featureless spin and dimer structure factors that indicate the absence of spin and dimer orders in the CSL state [57]. Next, we further characterize the nature of this CSL state.

Spontaneous time-reversal symmetry breaking. To detect spontaneous TRS breaking, we use a complex-valued wave function, which has been applied in DMRG to find chiral ground states in different systems [33,58]. If TRS is spontaneously broken, the system is featured by finite scalar chiral order $\langle \chi \rangle = \langle \mathbf{S}_1 \cdot (\mathbf{S}_2 \times \mathbf{S}_3) \rangle$, where \mathbf{S}_i (i = 1, 2, 3) label the three spins on each triangle. On the YC cylinder with both even and odd L_{v} , we find a nonzero chiral order in the bulk of cylinder with a large circumference, as shown in Fig. 2(a) for $J_2 = 0.3$, $J_3 = 0.15$. In these states, the chiral orders of all the up and down triangles have the same sign, and the chiral order grows more robust as the circumference increases. On the XC cylinder shown in Fig. 2(b), the chiral order vanishes in the bulk for small circumference but becomes stable on the wide XC12 cylinder. Combining these results we conclude a CSL state with spontaneous TRS breaking.

Spin triplet gap and entanglement characterization. We calculate the spin triplet gap by obtaining the ground state (in the S = 0 sector) on a long cylinder and then sweeping the S = 1 sector for the middle N_x columns [59], which gives the gap of the middle $N_x \times L_y$ system. We find that the gap versus $1/N_x$ shows a length dependence [57]. To estimate the gap in the two-dimensional (2D) limit and avoid one-dimensional (1D) physics, we extrapolate the gap data of the squarelike

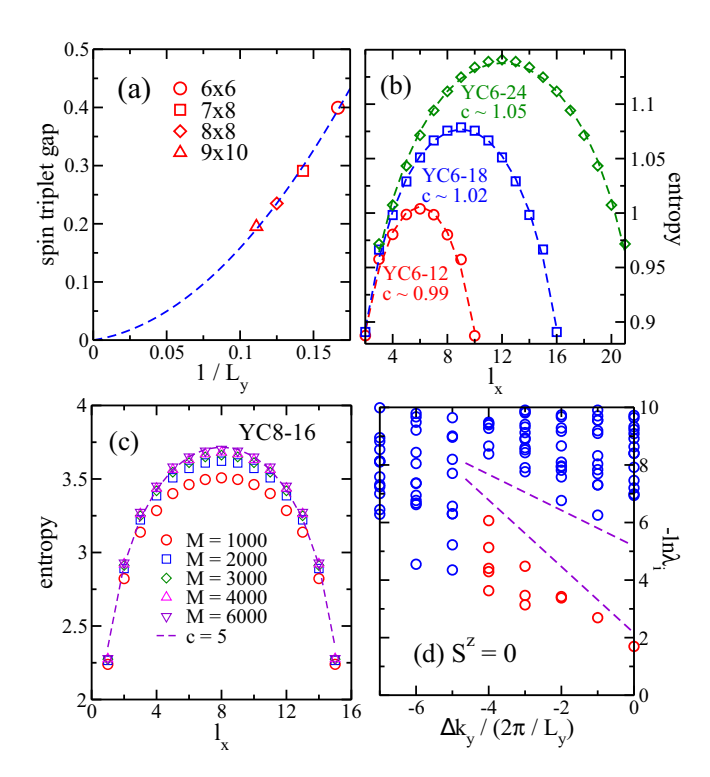


FIG. 3. (a) Size scaling of the spin triplet gap obtained on the squarelike clusters. (b) Entanglement entropy vs subsystem length l_x on the YC6 cylinders with different L_x . (c) Entanglement entropy on the YC8-16 cylinder by keeping different SU(2) state numbers. The dashed lines denote the fitting of entropy following the formula $S(l_x) = (c/6) \ln[(L_x/\pi) \sin(l_x\pi/L_x)] + g$, giving a central charge $c \simeq 1$ for the YC6 cylinder and $c \simeq 5$ for the YC8-16 cylinder. (d) Entanglement spectrum labeled by the quantum number total spin $S^z = 0$ and relative momentum along the y direction Δk_y . λ_i is the eigenvalue of the reduced density matrix. The red circles denote the near degenerate pattern $\{1, 1, 2, 3, 5\}$ of the low-lying spectrum.

clusters as shown in Fig. 3(a). The gap drops fast as a function of $1/L_y$ and smoothly scales to zero, suggesting gapless spintriplet excitations.

Furthermore, we study entanglement entropy versus subsystem length l_x by cutting the cylinder into two parts. Since the real-valued wave function is a superposition of the two chiral states with opposite chiralities, it has a higher entanglement entropy and is harder to converge to; thus we also use a complex-valued wave function to compute the entanglement entropy. As shown in Fig. 3(b) for $J_2 = 0.3$, $J_3 = 0.15$ on the YC6 cylinder, the entropy shows a logarithmic correction of the area law and follows the behavior $S(l_x) = (c/6) \ln[(L_x/\pi) \sin(l_x\pi/L_x)] + g$ [60], where $S(l_x)$ is the bipartite entanglement entropy, c is the central charge, and g is a nonuniversal constant. The YC6 cylinders with different L_x give a consistent central charge $c \simeq 1$. For the YC8 cylinder, we choose $L_x = 16$ (the entropy for larger L_x is much harder to converge and we show the results for $L_x = 24$ in the Supplemental Material [57], which are consistent with the fitted central charge c = 5). As shown in Fig. 3(c), the entropy continues to grow with a kept state number and converges very well by keeping 6000 SU(2) states, giving a large central charge of $c \simeq 5$. The finite central charge supports the gapless nature of the CSL state. Once a 2D quantum state is confined to a 1D cylinder, the finite circumference quantizes the momentum around the cylinder. The central charge of the 1D cylinder needs to sum over contributions from all quantized momenta. Taking the U(1)Dirac spin liquid as an example, the cylinder central charge c = 2 - 1 = 1 if the quantized momenta for each spin species only cross one Dirac cone, where the extra -1 accounts for the U(1) gauge field fluctuations which gaps out the total spinon density fluctuation [57,61]. Similarly $c \leq 3$ if the quantized momenta cross two Dirac cones (for each spin species), which is an upper bound for the central charge on a cylinder of any $L_{\rm v}$. The large central charge we found from DMRG is therefore inconsistent with the U(1) Dirac spin liquid on a triangular lattice [44,45,50], but provides strong evidence supporting emergent SFSs [14,15,18,19]. Now that each pair of crossings (one right mover and one left mover) between the quantized momenta and the SFSs contributes a unit of central charge, the total central charge of SFSs generally grows with L_v , with an upper bound of $c \leq N_w - 1$, where $2N_w$ is the total number of crossings [57].

For gapped CSL states, the entanglement spectrum has a one-to-one correspondence with the physical edge spectrum [62]. Interestingly, for this gapless CSL state the entanglement spectrum also shows a quasidegenerate group of levels with the counting $\{1, 1, 2, 3, 5, \ldots\}$ agreeing with chiral SU(2)₁ conformal field theory [63], as shown in Fig. 3(d). This may be an example of such states for an interacting system, which demonstrates similar edge physics as the noninteracting p + ip chiral superconductor with a gapless bulk spectrum [64,65].

The staggered flux state. To understand the DMRG results, we propose a staggered flux state, whose mean-field ansatz is constructed in the Abrikosov-fermion representation of spin- $\frac{1}{2}$ operators [66]

$$\mathbf{S}_{i} = \frac{1}{4} \operatorname{Tr}(\psi_{i}^{\dagger} \psi_{i} \boldsymbol{\sigma}^{T}), \quad \psi_{i} = \begin{pmatrix} f_{i,\uparrow} & f_{i,\downarrow} \\ f_{i,\downarrow}^{\dagger} & -f_{i,\uparrow}^{\dagger} \end{pmatrix}. \tag{2}$$

The Heisenberg Hamiltonian $H = \sum_{\langle ij \rangle} J_{ij} \mathbf{S}_i \cdot \mathbf{S}_j$ is decoupled into the mean-field form as

$$H_{\mathrm{MF}} = \frac{1}{8} \sum_{ij} J_{ij} \mathrm{Tr}(\psi_i^{\dagger} u_{ij} \psi_j + \mathrm{H.c.}) + \frac{1}{8} \sum_{ij} J_{ij} \mathrm{Tr}(u_{ij}^{\dagger} u_{ij}),$$

with the mean-field amplitude $u_{ij} = \langle \psi_i \psi_j^{\dagger} \rangle = u_{ij}^{\dagger}$. In the U(1) QSL states all spinon pairing terms will vanish and thus

$$u_{ij} = \begin{pmatrix} -\bar{\chi}_{ij} & 0\\ 0 & \chi_{ij} \end{pmatrix},\tag{3}$$

where $\chi_{ij}=\sum_{\alpha}\langle f_{i,\alpha}^{\dagger}f_{j,\alpha}\rangle=\bar{\chi}_{ji}$. Then the mean-field ansatz can be simplified as

$$H_{\mathbf{MF}} = \frac{J}{4} \sum_{\langle ij \rangle} \sum_{\alpha} (-\bar{\chi}_{ij} f_{i,\alpha}^{\dagger} f_{j,\alpha} + \text{H.c.}) + \frac{J}{4} \sum_{\langle ij \rangle} (|\chi_{ij}|^2),$$

where the mean-field ground state is at half filling due to the single-occupancy constraint on the parton Hilbert

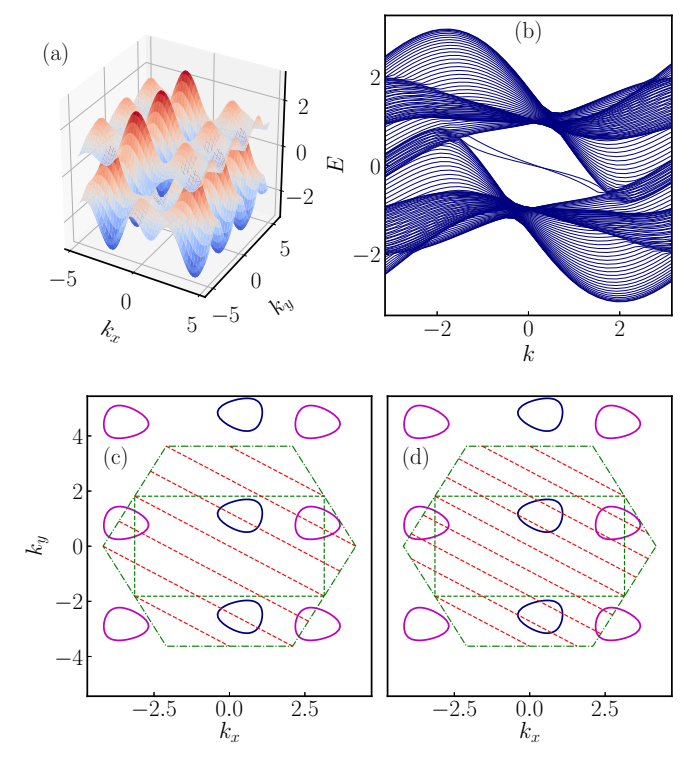


FIG. 4. Mean-field ansatz of the staggered flux state with up to third NN mean-field amplitudes. (a) Spinon dispersion. (b) Edge spectrum on a cylinder geometry. (c) and (d) show how the 1D channels with quantized momentum $k_2 = \frac{2\pi}{L_y} I_2$, $I_2 \in \mathbb{Z}$ cross the spinon Fermi surfaces (SFSs) on finite YC cylinders with $L_y = 6$, 8. The dotted rectangle is the reduced Brillouin zone due to the doubling of unit cell in the mean-field ansatz. Pink and blue circles denote holeand particlelike SFSs, respectively.

space

$$\sum_{\alpha=\uparrow,\downarrow} f_{i\alpha}^{\dagger} f_{i\alpha} = 1, \ \forall i.$$
 (4)

We consider a U(1) spin liquid known as the staggered flux state [67–69], where fermionic spinons transform under translations as follows,

$$f_{\mathbf{r},\alpha} \xrightarrow{T_2} (-)^{r_1} f_{\mathbf{r}+\mathbf{a}_1,\alpha}^{\dagger}, \quad f_{\mathbf{r},\alpha} \xrightarrow{T_1} f_{\mathbf{r}+\mathbf{a}_1,\alpha}.$$
 (5)

Although the mean-field ansatz doubles the unit cell (along the \mathbf{a}_2 direction), the projected wave function preserves the lattice translation symmetries by $\mathbf{a}_{1,2}$.

Since the spin model has couplings up to the third NN sites, we consider the symmetry-allowed mean-field ansatz with hopping terms up to the third NN, which are shown in the Supplemental Material [57]. The NN hopping ansatz reduces to the π -flux U(1) QSL state [50] in the case of $\phi_1 = \phi_2 = \pi/2$ (ϕ_1, ϕ_2 are the phases of the NN hoppings), with a pair of Dirac spinons at half filling for each spin species. The second and third NN hoppings can open up a direct gap at each Dirac cone, leading to a Chern number $C = \pm 1$ of the lower spinon band and the chiral edge states shown in Fig. 4(b). Meanwhile the third NN hoppings can break the degeneracy of two Dirac cones, giving rise to one particlelike SFS around one Dirac point [blue in Figs. 4(c)

and 4(d)] and a holelike SFS around the other Dirac point [pink in Figs. 4(c) and 4(d)]. Due to the single-occupancy constraint Eq. (4), the particlelike SFS and holelike SFS are perfectly compensated at half filling. Choosing mean-field parameters as $\chi = 1.0$, $\phi_1 = \phi_2 = \pi/2$, $\lambda = 1.0$, $\varphi_1 = \varphi_2 = \varphi_3 = 0$, $\rho = 3.0$, $\gamma_1 = \gamma_2 = \gamma_3 = \pi/2$ [57], the mean-field dispersion and edge spectrum of fermionic spinons are shown in Figs. 4(a) and 4(b).

For further comparison with DMRG, we follow the YC cylinder geometry with quantized momentum $k_2 = 2\pi l_2/L_y$ along the \mathbf{b}_2 direction. In Figs. 4(c) and 4(d) we depict how the 1D channels with quantized momenta $k_2 = 2\pi l_2/L_y$ intersect with the two SFSs in the reduced Brillouin zone of the staggered flux state. On the YC6 cylinder, as shown in Fig. 4(c), there are $N_w = 2 \times 2 = 4$ pairs of gapless 1D modes crossing the SFSs (counting both spin species), constraining the central charge to be $c \leq N_w - 1 = 3$. On the YC8 cylinder, as shown in Fig. 4(d), there are $N_w = 2 \times 4 = 8$ pairs of gapless 1D modes crossing the SFSs, restricting the central charge as $c \leq N_w - 1 = 7$. This is consistent with the observed $c \approx 1$ on YC6-24 cylinder [Fig. 3(b)] and $c \approx 5$ on YC8-16 cylinder [Fig. 3(c)]. Note that the number $N_w - 1$ only bound the actual central charge from above, since symmetric backscatterings between these gapless 1D channels can further reduce the total central charge from $N_w - 1$ [57].

Discussion. The spin structure factor of the gapless CSL phase in Fig. 1(b) resembles that of the U(1) Dirac spin liquid [45]. Specifically, it exhibits high intensities on the edge and at the corner of the hexagonal Brillouin zone, which are associated with fermion bilinears and monopoles, respectively, in the U(1) Dirac spin liquid [70,71]. This suggests the proximity of the gapless CSL to the U(1) Dirac state, which is indeed the case for the proposed staggered flux state. We have also studied the phase transition from the J_1 - J_2 SL phase to the gapless CSL phase. The ground-state energy versus couplings is very smooth, suggesting a possible continuous phase transition [57]. Interestingly, in the J_1 - J_2 SL entanglement entropy also shows a logarithmic correction of the area law, which leads to a finite central charge [57]. Another insight for its ground state could be a gapless spin liquid with SFSs but preserving TRS, which we leave for future work.

Summary. We have studied the spin- $\frac{1}{2}J_1$ - J_2 - J_3 THM by extensive DMRG calculations. We identify a CSL state spontaneously breaking TRS, featuring a chiral edge mode and spin pumping upon flux insertion. The vanishing spin triplet gap and finite central charge reveal the gapless nature of this state. The central charge which grows with system circumference further indicates emergent SFSs. While the competing J_2, J_3 couplings lead to a gapped CSL on a kagome lattice [34,72], they induce a gapless CSL on a triangular lattice. On the mean-field level we propose a staggered flux state driven by the J_2 , J_3 couplings, which breaks TRS and forms SFS, providing a theoretical understanding for such a gapless phase. The discovery of this gapless CSL reveals the possibility for the coexistence of chiral edge modes and SFSs in a gapless QSL, emergent from competing interactions in a frustrated two-dimensional magnet.

Note added. Recently, we became aware of an article by Hu *et al.* [73], who studied the J_1 - J_2 spin liquid. Compared

to their work, our work focuses on the J_1 - J_2 - J_3 model and found a staggered flux state driven by further-neighbor interactions.

Acknowledgments. We would like to thank Olexei I. Motrunich, Tao Li, and Yuan Wan for extensive discussions. S.S.G. is supported by the National Natural Science Foundation of China (Grants No. 11874078 and No. 11834014) and

the Fundamental Research Funds for the Central Universities. M.L. is supported by the National Science Foundation through PREM Grant No. DMR-1828019. D.N.S. is supported by the U.S. Department of Energy, Office of Basic Energy Sciences under Grant No. DE-FG02-06ER46305. W.Z. and Y.M.L. are supported by National Science Foundation under Award No. DMR-1653769.

- [1] L. Balents, Spin liquids in frustrated magnets, Nature (London) 464, 199 (2010).
- [2] L. Savary and L. Balents, Quantum spin liquids: A review, Rep. Prog. Phys. 80, 016502 (2016).
- [3] Y. Zhou, K. Kanoda, and T.-K. Ng, Quantum spin liquid states, Rev. Mod. Phys. 89, 025003 (2017).
- [4] X. G. Wen, Mean-field theory of spin-liquid states with finite energy gap and topological orders, Phys. Rev. B 44, 2664 (1991).
- [5] T. Senthil and M. P. A. Fisher, Z₂ gauge theory of electron fractionalization in strongly correlated systems, Phys. Rev. B 62, 7850 (2000).
- [6] T. Senthil and M. P. A. Fisher, Fractionalization in the Cuprates: Detecting the Topological Order, Phys. Rev. Lett. 86, 292 (2001).
- [7] X.-G. Wen, Topological order: From long-range entangled quantum matter to a unified origin of light and electrons, ISRN Condens. Matter Phys. 2013, 198710 (2013).
- [8] P. W. Anderson, Resonating valence bonds: A new kind of insulator? Mater. Res. Bull. **8**, 153 (1973).
- [9] N. Read and S. Sachdev, Large-N Expansion for Frustrated Quantum Antiferromagnets, Phys. Rev. Lett. 66, 1773 (1991).
- [10] S. Sachdev, Kagome and triangular-lattice Heisenberg antiferromagnets: Ordering from quantum fluctuations and quantumdisordered ground states with unconfined bosonic spinons, Phys. Rev. B 45, 12377 (1992).
- [11] P. A. Lee, N. Nagaosa, and X.-G. Wen, Doping a Mott insulator: Physics of high-temperature superconductivity, Rev. Mod. Phys. **78**, 17 (2006).
- [12] A. Kitaev, Anyons in an exactly solved model and beyond, Ann. Phys. **321**, 2 (2006).
- [13] M. Hermanns, I. Kimchi, and J. Knolle, Physics of the Kitaev model: Fractionalization, dynamic correlations, and material connections, Annu. Rev. Condens. Matter Phys. 9, 17 (2018).
- [14] L. B. Ioffe and A. I. Larkin, Gapless fermions and gauge fields in dielectrics, Phys. Rev. B 39, 8988 (1989).
- [15] N. Nagaosa and P. A. Lee, Normal-State Properties of the Uniform Resonating-Valence-Bond State, Phys. Rev. Lett. 64, 2450 (1990).
- [16] P. A. Lee and N. Nagaosa, Gauge theory of the normal state of high-*T_c* superconductors, Phys. Rev. B **46**, 5621 (1992).
- [17] G. Misguich, C. Lhuillier, B. Bernu, and C. Waldtmann, Spinliquid phase of the multiple-spin exchange Hamiltonian on the triangular lattice, Phys. Rev. B 60, 1064 (1999).
- [18] O. I. Motrunich, Variational study of triangular lattice spin-1/2 model with ring exchanges and spin liquid state in κ -(ET)₂Cu₂(CN)₃, Phys. Rev. B **72**, 045105 (2005).

- [19] D. N. Sheng, O. I. Motrunich, and M. P. A. Fisher, Spin Bose-metal phase in a spin-½ model with ring exchange on a two-leg triangular strip, Phys. Rev. B **79**, 205112 (2009).
- [20] M. S. Block, D. N. Sheng, O. I. Motrunich, and M. P. A. Fisher, Spin Bose-Metal and Valence Bond Solid Phases in a Spin-1/2 Model with Ring Exchanges on a Four-Leg Triangular Ladder, Phys. Rev. Lett. 106, 157202 (2011).
- [21] W.-Y. He, X. Y. Xu, G. Chen, K. T. Law, and P. A. Lee, Spinon Fermi Surface in a Cluster Mott Insulator Model on a Triangular Lattice and Possible Application to 1*T*-TaS₂, Phys. Rev. Lett. 121, 046401 (2018).
- [22] Y. Shimizu, K. Miyagawa, K. Kanoda, M. Maesato, and G. Saito, Spin Liquid State in an Organic Mott Insulator with a Triangular Lattice, Phys. Rev. Lett. 91, 107001 (2003).
- [23] Y. Kurosaki, Y. Shimizu, K. Miyagawa, K. Kanoda, and G. Saito, Mott Transition from a Spin Liquid to a Fermi Liquid in the Spin-Frustrated Organic Conductor κ-(ET)₂Cu₂(CN)₃, Phys. Rev. Lett. 95, 177001 (2005).
- [24] S. Yamashita, Y. Nakazawa, M. Oguni, Y. Oshima, H. Nojiri, Y. Shimizu, K. Miyagawa, and K. Kanoda, Thermodynamic properties of a spin-1/2 spin-liquid state in a κ-type organic salt, Nat. Phys. 4, 459 (2008).
- [25] M. Yamashita, N. Nakata, Y. Kasahara, T. Sasaki, N. Yoneyama, N. Kobayashi, S. Fujimoto, T. Shibauchi, and Y. Matsuda, Thermal-transport measurements in a quantum spin-liquid state of the frustrated triangular magnet κ -(BEDT-TTF)₂Cu₂(CN)₃, Nat. Phys. **5**, 44 (2009).
- [26] M. Yamashita, N. Nakata, Y. Senshu, M. Nagata, H. M. Yamamoto, R. Kato, T. Shibauchi, and Y. Matsuda, Highly mobile gapless excitations in a two-dimensional candidate quantum spin liquid, Science 328, 1246 (2010).
- [27] K. T. Law and P. A. Lee, 1*T*-TaS₂ as a quantum spin liquid, Proc. Natl. Acad. Sci. USA **114**, 6996 (2017).
- [28] Y. J. Yu, Y. Xu, L. P. He, M. Kratochvilova, Y. Y. Huang, J. M. Ni, L. Wang, S.-W. Cheong, J.-G. Park, and S. Y. Li, Heat transport study of the spin liquid candidate 1*T*-TaS₂, Phys. Rev. B 96, 081111(R) (2017).
- [29] A. Ribak, I. Silber, C. Baines, K. Chashka, Z. Salman, Y. Dagan, and A. Kanigel, Gapless excitations in the ground state of 1*T*-TaS₂, Phys. Rev. B 96, 195131 (2017).
- [30] M. Klanjšek, A. Zorko, R. Žitko, J. Mravlje, Z. Jagličić, P. K. Biswas, P. Prelovšek, D. Mihailovic, and D. Arčon, A high-temperature quantum spin liquid with polaron spins, Nat. Phys. 13, 1130 (2017).
- [31] A. Szasz, J. Motruk, M. P. Zaletel, and J. E. Moore, Observation of a chiral spin liquid phase of the Hubbard model on the

- triangular lattice: A density matrix renormalization group study, arXiv:1808.00463.
- [32] B. Fåk, E. Kermarrec, L. Messio, B. Bernu, C. Lhuillier, F. Bert, P. Mendels, B. Koteswararao, F. Bouquet, J. Ollivier, A. D. Hillier, A. Amato, R. H. Colman, and A. S. Wills, Kapellasite: A Kagome Quantum Spin Liquid with Competing Interactions, Phys. Rev. Lett. 109, 037208 (2012).
- [33] S.-S. Gong, W. Zhu, and D. N. Sheng, Emergent chiral spin liquid: Fractional quantum Hall effect in a kagome Heisenberg model, Sci. Rep. 4, 6317 (2014).
- [34] S.-S. Gong, W. Zhu, L. Balents, and D. N. Sheng, Global phase diagram of competing ordered and quantum spin-liquid phases on the kagome lattice, Phys. Rev. B **91**, 075112 (2015).
- [35] J. A. M. Paddison, M. Daum, Z. Dun, G. Ehlers, Y. Liu, M. B. Stone, H. Zhou, and M. Mourigal, Continuous excitations of the triangular-lattice quantum spin liquid YbMgGaO₄, Nat. Phys. 13, 117 (2017).
- [36] Z. Zhu, P. A. Maksimov, S. R. White, and A. L. Chernyshev, Topography of Spin Liquids on a Triangular Lattice, Phys. Rev. Lett. 120, 207203 (2018).
- [37] X. Zhang, F. Mahmood, M. Daum, Z. Dun, J. A. M. Paddison, N. J. Laurita, T. Hong, H. Zhou, N. P. Armitage, and M. Mourigal, Hierarchy of Exchange Interactions in the Triangular-Lattice Spin Liquid YbMgGaO₄, Phys. Rev. X 8, 031001 (2018).
- [38] Y. Li, G. Chen, W. Tong, L. Pi, J. Liu, Z. Yang, X. Wang, and Q. Zhang, Rare-Earth Triangular Lattice Spin Liquid: A Single-Crystal Study of YbMgGaO₄, Phys. Rev. Lett. **115**, 167203 (2015).
- [39] Y. Shen, Y.-D. Li, H. C. Walker, P. Steffens, M. Boehm, X. Zhang, S. Shen, H. Wo, G. Chen, and J. Zhao, Fractionalized excitations in the partially magnetized spin liquid candidate YbMgGaO₄, Nat. Commun. 9, 4138 (2018).
- [40] T. Kimura, J. C. Lashley, and A. P. Ramirez, Inversion-symmetry breaking in the noncollinear magnetic phase of the triangular-lattice antiferromagnet CuFeO₂, Phys. Rev. B **73**, 220401(R) (2006).
- [41] F. Ye, J. A. Fernandez-Baca, R. S. Fishman, Y. Ren, H. J. Kang, Y. Qiu, and T. Kimura, Magnetic Interactions in the Geometrically Frustrated Triangular Lattice Antiferromagnet CuFeO₂, Phys. Rev. Lett. 99, 157201 (2007).
- [42] H. Kadowaki, H. Kikuchi, and Y. Ajiro, Neutron powder diffraction study of the two-dimensional triangular lattice antiferromagnet CuCrO₂, J. Phys.: Condens. Matter **2**, 4485 (1990).
- [43] S. Seki, Y. Onose, and Y. Tokura, Spin-Driven Ferroelectricity in Triangular Lattice Antiferromagnets *A*CrO₂ (*A* = Cu, Ag, Li, or Na), Phys. Rev. Lett. **101**, 067204 (2008).
- [44] R. Kaneko, S. Morita, and M. Imada, Gapless spin-liquid phase in an extended spin 1/2 triangular Heisenberg model, J. Phys. Soc. Jpn. 83, 093707 (2014).
- [45] Y. Iqbal, W.-J. Hu, R. Thomale, D. Poilblanc, and F. Becca, Spin liquid nature in the Heisenberg $J_1 J_2$ triangular antiferromagnet, Phys. Rev. B **93**, 144411 (2016).
- [46] P. H. Y. Li, R. F. Bishop, and C. E. Campbell, Quasiclassical magnetic order and its loss in a spin- $\frac{1}{2}$ Heisenberg antiferromagnet on a triangular lattice with competing bonds, Phys. Rev. B **91**, 014426 (2015).
- [47] Z. Zhu and S. R. White, Spin liquid phase of the $s = \frac{1}{2}J_1 J_2$ Heisenberg model on the triangular lattice, Phys. Rev. B **92**, 041105(R) (2015).

- [48] W.-J. Hu, S.-S. Gong, W. Zhu, and D. N. Sheng, Competing spin-liquid states in the spin- $\frac{1}{2}$ Heisenberg model on the triangular lattice, Phys. Rev. B **92**, 140403(R) (2015).
- [49] W. Zheng, J.-W. Mei, and Y. Qi, Classification and Monte Carlo study of symmetric Z₂ spin liquids on the triangular lattice, arXiv:1505.05351.
- [50] Y.-M. Lu, Symmetric Z_2 spin liquids and their neighboring phases on triangular lattice, Phys. Rev. B **93**, 165113 (2016).
- [51] S. N. Saadatmand and I. P. McCulloch, Symmetry fractionalization in the topological phase of the spin-1/2 $J_1 J_2$ triangular Heisenberg model, Phys. Rev. B **94**, 121111(R) (2016).
- [52] N. B. Ivanov and J. Richter, Spiral phases in easy plane $J_1 J_2 J_3$ triangular antiferromagnets, J. Magn. Magn. Mater. **140-144**, 1965 (1995).
- [53] N. Y. Yao, M. P. Zaletel, D. M. Stamper-Kurn, and A. Vishwanath, A quantum dipolar spin liquid, Nat. Phys. 14, 405 (2018).
- [54] J. Iaconis, C. Liu, G. B. Halász, and L. Balents, Spin liquid versus spin orbit coupling on the triangular lattice, SciPost Phys. 4, 003 (2018).
- [55] S. R. White, Density Matrix Formulation for Quantum Renormalization Groups, Phys. Rev. Lett. 69, 2863 (1992).
- [56] I. McCulloch and M. Gulácsi, The non-Abelian density matrix renormalization group algorithm, Europhys. Lett. 57, 852 (2002).
- [57] See Supplemental Material at http://link.aps.org/supplemental/ 10.1103/PhysRevB.100.241111 for more details.
- [58] W. Zhu, S.-S. Gong, T.-S. Zeng, L. Fu, and D. N. Sheng, Interaction-Driven Spontaneous Quantum Hall Effect on a Kagome Lattice, Phys. Rev. Lett. 117, 096402 (2016).
- [59] S. Yan, D. A. Huse, and S. R. White, Spin-liquid ground state of the S = 1/2 kagome Heisenberg antiferromagnet, Science **332**, 1173 (2011).
- [60] P. Calabrese and J. Cardy, Entanglement entropy and quantum field theory, J. Stat. Mech.: Theory Exp. (2004) P06002.
- [61] S. D. Geraedts, M. P. Zaletel, R. S. K. Mong, M. A. Metlitski, A. Vishwanath, and O. I. Motrunich, The half-filled Landau level: The case for Dirac composite fermions, Science 352, 197 (2016).
- [62] H. Li and F. D. M. Haldane, Entanglement Spectrum as a Generalization of Entanglement Entropy: Identification of Topological Order in Non-Abelian Fractional Quantum Hall Effect States, Phys. Rev. Lett. 101, 010504 (2008).
- [63] P. Francesco, P. Mathieu, and D. Sénéchal, Conformal Field Theory (Springer, Berlin, 2012).
- [64] J. Dubail and N. Read, Tensor network trial states for chiral topological phases in two dimensions and a no-go theorem in any dimension, Phys. Rev. B 92, 205307 (2015).
- [65] D. Poilblanc, Investigation of the chiral antiferromagnetic Heisenberg model using projected entangled pair states, Phys. Rev. B **96**, 121118(R) (2017).
- [66] A. A. Abrikosov, Electron scattering on magnetic impurities in metals and anomalous resistivity effects, Physics 2, 5 (1965).
- [67] X.-G. Wen, Quantum orders and symmetric spin liquids, Phys. Rev. B 65, 165113 (2002).
- [68] Y.-D. Li, Y.-M. Lu, and G. Chen, Spinon fermi surface U(1) spin liquid in the spin-orbit-coupled triangular-lattice Mott insulator YbMgGaO₄, Phys. Rev. B **96**, 054445 (2017).

- [69] S. Bieri, C. Lhuillier, and L. Messio, Projective symmetry group classification of chiral spin liquids, Phys. Rev. B 93, 094437 (2016).
- [70] X.-Y. Song, C. Wang, A. Vishwanath, and Y.-C. He, Unifying description of competing orders in two dimensional quantum magnets, Nature Commun. **10**, 4254 (2019).
- [71] X.-Y. Song, Y.-C. He, A. Vishwanath, and C. Wang, From spinon band topology to the symmetry
- quantum numbers of monopoles in Dirac spin liquids, arXiv:1811.11182.
- [72] Y.-C. He, D. N. Sheng, and Y. Chen, Chiral Spin Liquid in a Frustrated Anisotropic Kagome Heisenberg Model, Phys. Rev. Lett. **112**, 137202 (2014).
- [73] S. Hu, W. Zhu, S. Eggert, and Y.-C. He, Dirac Spin Liquid on the Spin-1/2 Triangular Heisenberg Antiferromagnet, Phys. Rev. Lett. **123**, 207203 (2019).